Time-migration in the Common-Reflection-Point (CRP) domain

Tiago A. Coimbra* (CEPETRO/UNICAMP), Jorge H. Faccipieri (CEPETRO/UNICAMP) and Martin Tygel (IMECC/UNICAMP)

This paper was prepared for presentation at the 14th International Congress of the Brazilian Geophysical Society, held in Rio de Janeiro, Brazil, August 3-6, 2015.

Abstract

Since the early days of seismic processing, time migration has proven to be a valuable tool for a number of imaging purposes. Main motivations for its widespread use include robustness with respect to velocity errors, as well as fast turnovers and low computation costs. In areas of complex geology, in which it has well-known limitations, time migration can still be of value by providing first images and also attributes that help in further imaging tasks, such as depth migration. Application of the zero-offset (ZO) common reflection surface (CRS) method to prestack data can be much beneficial to time migration, since Kirchhoff traveltime operators can be naturally constructed from the attributes (CRS parameters) that result from the CRS application. In the nineties, several studies have shown appealing advantages in the use of common-reflection-point (CRP) traveltimes to replace conventional diffraction-stack operators for a number of stacking and migration purposes. In this paper, we follow this path introducing a Kirchhoff-type prestack time migration algorithm that uses CRP stacking operator. The proposed CRP operator, together with optimal apertures, is also computed with the help of CRS parameters. Field data example indicate the good potential of the proposed approach.

Introduction

Time migration is an obligatory step in practically all seismic processing in the oil industry. Roughly speaking, time migration simulates the illumination of reflectors and scatterers by means of ”zero-offset (ZO) image rays”, which start with slowness vector perpendicular to the acquisition surface and returns to that surface along the same path (see, e.g., Hubral and Krey, 1980; Yilmaz, 2001). Advantages of time migration include, besides robustness (less sensitivity to velocity errors), fast turnovers and low computational costs, also collapse of diffractions and absence of conflicting dips. In fact, in many situations (typically mild to moderate laterally velocity variations), time-migrated images can be sufficient for satisfactory interpretation. Losses in image accuracy and interpretation power (mainly associated with geological complexity and strong lateral velocity variations) are well-known limitations of time migration, as compared to comprehensive depth migration. Because of noise reduction, collapse of diffractions and triplications, time-migrated images can be also of help in event picking, seismic tomography (Dell et al., 2014), as well as time-to-depth conversion (Cameron et al., 2007; Iversen and Tygel, 2008).

The good properties of time migration motivates the search of more accurate algorithms to overcome limitations and enlarge the applicability of time migration. As shown in the literature (Perroud et al., 1999; Spinner and Mann, 2006; Coimbra et al., 2011, 2013), it is advantageous to replace the conventional time-migration diffraction-stack operators by appropriate common-reflection-point (CRP) operators, the latter being constructed, typically with common-reflection-surface (CRS) parameters. Moreover, additional accuracy is also obtained by considering minimum apertures, defined in terms of projected Fresnel zones (PFZ)(Schleicher et al., 1997; Faccipieri et al., 2015). Such apertures are also estimated using CRS parameters.

In this paper, we follow the trend of performing Kirchhoff-type, time migration under the use of CRP operators and optimal apertures, both computed with the help of CRS parameters. The approach is called CRP time migration. Besides describing the proposed technique, we briefly discuss and compare the proposed technique with the conventional Kirchhoff approach of widespread practical use. A field data example confirms the good potential of the proposed technique for accurate time migration.

Formulation

The CRP time migration technique envisaged here is formulated as a Kirchhoff-type algorithm, in which the migration operator is a CRP traveltime, that is expressed in terms of CRS parameters estimated from the prestack data. Furthermore, the same CRS parameters also define a minimal aperture in which the Kirchhoff summation is optimally carried out.

The construction of the proposed CRP time migration is based on the relationships between the traveltime operators of stacking (here represented by the ZO CRS diffraction traveltime) and time migration (here represented by the double-square root (DSR) traveltime), both operators referring to the same (unknown) target reflector. For simplicity, we assume that the acquisition surface is planar horizontal.

Notation

Both operators are defined on a same prestack data volume, with traces specified as $(\mathbf{m},\mathbf{h})$, in which $\mathbf{m} = (m_1,m_2)^T$ and $\mathbf{h} = (h_1,h_2)^T$ represent midpoint and half-offset coordinates. As usual practice, we assume that the application of the stacking operator produces a data volume that well approximates a ZO volume, namely the one that would be obtained if the subsurface were illuminated by a ZO acquisition. In the same way, the application of the time-migration operator produces a prestack Kirchhoff time-migrated image of that subsurface.

The central point of the stacking operator (i.e., the point where the stacking output is assigned) is denoted by $(\mathbf{m}_0, t_0)$, in which $\mathbf{m}_0 = (m_{01}, m_{02})^T$ represents trace location and t_0 the traveltime in the ZO (stacked) domain. More specifically, t_0 represents the two-way traveltime of the ZO reflection ray (assumed non-converted primary) from the surface point specified by $\mathbf{m}_0$ to the target reflector. That ZO (normal) ray is called the central ray and supposed to be uniquely determined by $\mathbf{m}_0$. The point where the ZO central ray hits the target reflector is referred to as the normal-incidence point (NIP).

In the same way, the central point of the time migration operator (i.e., the point where the time migration output is assigned) is denoted by $(\mathbf{x}_0, \tau_0)$, in which $\mathbf{x}_0 = (x_{01}, x_{02})^T$ represents trace location and τ_0 is the two-way traveltime in the time migrated domain. The point at the surface specified by $\mathbf{x}_0$ is determined from the central image ray, which is the one that starts at NIP on the target reflector and hits the surface with slowness vector perpendicular to that surface.

Stacking and time migration operators:

With the notations described above, we are ready to write the stacking and time-migration operators under consideration. We recall that such operators are linked to the same (unknown) target reflector. More specifically, the central points $(\mathbf{m}_0, t_0)$ and $(\mathbf{x}_0, \tau_0)$ of the stacked and time migration operators relates to the same NIP at the target reflector by means of the central ZO and image rays, respectively. We have

(a) Stacking operator: That is given by the ZO CRS diffraction moveout, defined in the prestack domain and central point, $(\mathbf{m}_0, t_0)$ at the ZO (stacked) volume,

$$t_D(\mathbf{m}, \mathbf{h}) = \sqrt{(t_0 + \mathbf{a}^T \Delta\mathbf{m})^2 + \Delta\mathbf{m}^T \mathbf{C} \Delta\mathbf{m} + \mathbf{h}^T \mathbf{C} \mathbf{h}}\,, \quad (1)$$

where we introduce the notation $\Delta\mathbf{m} = \mathbf{m} - \mathbf{m}_0$. In the above equation, the coefficients (CRS parameters) are given by

$$\mathbf{a} = \left[\frac{\partial t}{\partial m_i}\right]_{(\mathbf{m}_0, \mathbf{0})}, \; \mathbf{C} = t_0 \left[\frac{\partial^2 t}{\partial h_i \partial h_j}\right]_{(\mathbf{m}_0, \mathbf{0})}, \; i, j = 1, 2. \quad (2)$$

(b) Time-migration operator: That is given by the double-square-root (DSR) moveout, defined in the prestack domain and of central point $(\mathbf{x}_0, \tau_0)$ in the time-migrated domain

$$\begin{aligned} t_M(\mathbf{m}, \mathbf{h}) &= \frac{1}{2}\sqrt{\tau_0^2 + (\mathbf{m} - \mathbf{h} - \mathbf{x}_0)^T \mathbf{S} (\mathbf{m} - \mathbf{h} - \mathbf{x}_0)} \\ &+ \frac{1}{2}\sqrt{\tau_0^2 + (\mathbf{m} + \mathbf{h} - \mathbf{x}_0)^T \mathbf{S} (\mathbf{m} + \mathbf{h} - \mathbf{x}_0)}, \end{aligned} \quad (3)$$

where the coefficient (migration parameter) is given by

$$\mathbf{S} = \tau_0 \left[\frac{\partial^2 \tau}{\partial x_i \partial x_j}\right]_{(\mathbf{x}_0)}, \quad i, j = 1, 2. \quad (4)$$

In the literature, the time-migration matrix, $\mathbf{S}$, is referred to as the *sloth parameter*. For later use, it is convenient to write down the above traveltimes in the ZO configuration, namely $t_{ZO}^D(\mathbf{m}) = t_D(\mathbf{m}, \mathbf{0})$ and $t_{ZO}^M(\mathbf{m}) = t_M(\mathbf{m}, \mathbf{0})$. After a little algebra, we find

$$[t_{ZO}^D(\mathbf{m})]^2 = t_0^2 + 2t_0 \mathbf{a}^T \Delta\mathbf{m} + \Delta\mathbf{m}^T (\mathbf{a}\mathbf{a}^T + \mathbf{C}) \Delta\mathbf{m}\,, \quad (5)$$

$$[t_{ZO}^M(\mathbf{m})]^2 = \tau_0^2 + (\mathbf{m} - \mathbf{x}_0)^T \mathbf{S} (\mathbf{m} - \mathbf{x}_0)\,. \quad (6)$$

Relationships between coefficients of stacking and time migration operators

We now investigate the link between the coefficients of the stacking and time migration operators related to the same target reflector. For that, we consider stacking and time-migration ZO operators of Equations (5) and (6).

We suppose that the the central point $(\mathbf{m}_0, t_0)$ of the stacking operator is a reflection point in the ZO (stacked) domain and, moreover, that point mapped to $(\mathbf{x}_0, \tau_0)$ after time migration. Following Mann et al. (2000) (in the 2D situation) and Gelius and Tygel (2015) (in the 3D case), we recall that the time-migrated point, $(\mathbf{x}_0, \tau_0)$, that corresponds to the ZO point $(\mathbf{m}_0, t_0)$, is the minimum (apex) of the stacking operator, $t_{ZO}^D(\mathbf{m})$. As such, that apex, $\mathbf{m} = \mathbf{x}_0$, is determined by the condition

$$\begin{aligned} \left.\frac{\partial [t_{ZO}^D]^2}{\partial \mathbf{m}}\right|_{\mathbf{m}=\mathbf{x}_0} &= 2t_{ZO}^D(\mathbf{x}_0) \left.\frac{\partial t_{ZO}^D}{\partial \mathbf{m}}\right|_{\mathbf{m}=\mathbf{x}_0} \\ &= 2[t_0 \mathbf{a} + (\mathbf{a}\mathbf{a}^T + \mathbf{C})(\mathbf{x}_0 - \mathbf{m}_0)] = 0\,. \end{aligned} \quad (7)$$

Solving for $\mathbf{m}_0$ and substituting into Equation (5), leads to the expressions

$$\mathbf{x}_0 = \mathbf{m}_0 - t_0 (\mathbf{a}\mathbf{a}^T + \mathbf{C})^{-1} \mathbf{a}\,, \quad (8)$$

$$\tau_0 = t_{ZO}^D(\mathbf{x}_0) = t_0 \sqrt{1 - \mathbf{a}^T (\mathbf{a}\mathbf{a}^T + \mathbf{C})^{-1} \mathbf{a}}\,. \quad (9)$$

Moreover, we also find the relation

$$t_{ZO}^D(\mathbf{m})^2 = \tau_0^2 + (\mathbf{m} - \mathbf{x}_0)^T \left(\mathbf{a}\mathbf{a}^T + \mathbf{C}\right) (\mathbf{m} - \mathbf{x}_0)\,, \quad (10)$$

from which, comparison with the ZO time-migration operator $t_{ZO}^M(\mathbf{m})$ of Equation (6) leads to the additional relations

$$\mathbf{S} = \mathbf{a}\mathbf{a}^T + \mathbf{C}\,, \quad (11)$$

$$t_0^2 = [t_{ZO}^M(\mathbf{m}_0)]^2 = \tau_0^2 + (\mathbf{m}_0 - \mathbf{x}_0)^T \mathbf{S} (\mathbf{m}_0 - \mathbf{x}_0)\,. \quad (12)$$

We finally observe that

$$\mathbf{C} = 4\mathbf{V}_{NMO}^{-2}, \quad \text{and} \quad \mathbf{S} = 4\mathbf{V}_M^{-2}\,, \quad (13)$$

where $\mathbf{V}_{NMO}$ and $\mathbf{V}_M$ are the so-called NMO and time migration velocity ellipses, evaluated at $(\mathbf{m}_0, t_0)$ and $(\mathbf{x}_0, \tau_0)$, respectively. We note that, in the 2D situation, V_{NMO} and V_M represent the NMO and time migration velocities, respectively.

Expression of the CRP trajectory

We now focus on the construction of the CRP operator that refers to a given time-migration sloth parameter, $\mathbf{S}$ and time-migration central point, $(\mathbf{x}_0, \tau_0)$. For that, we start with the time-migration operator of Equation (3) for a fixed half-offset, $\mathbf{h}$, which we recast in the more convenient form

$$t_M(\mathbf{m},\mathbf{h};\mathbf{x}_0,\tau_0) = t_s(\mathbf{m},\mathbf{h};\mathbf{x}_0,\tau_0) + t_g(\mathbf{m},\mathbf{h};\mathbf{x}_0,\tau_0)\,, \qquad (14)$$

with $t_s = t_s(\mathbf{m},\mathbf{h};\mathbf{x}_0,\tau_0)$ and $t_g = t_g(\mathbf{m},\mathbf{h};\mathbf{x}_0,\tau_0)$ given by

$$t_s^2 = \frac{\tau_0^2}{4} + \frac{1}{4}(\mathbf{m}-\mathbf{h}-\mathbf{x}_0)^T\mathbf{S}(\mathbf{m}-\mathbf{h}-\mathbf{x}_0)\,, \qquad (15)$$

$$t_g^2 = \frac{\tau_0^2}{4} + \frac{1}{4}(\mathbf{m}+\mathbf{h}-\mathbf{x}_0)^T\mathbf{S}(\mathbf{m}+\mathbf{h}-\mathbf{x}_0)\,. \qquad (16)$$

Note the change in notation in the above expressions, for which the dependence on the time-migration central point, $(\mathbf{x}_0, \tau_0)$, is made explicitly.

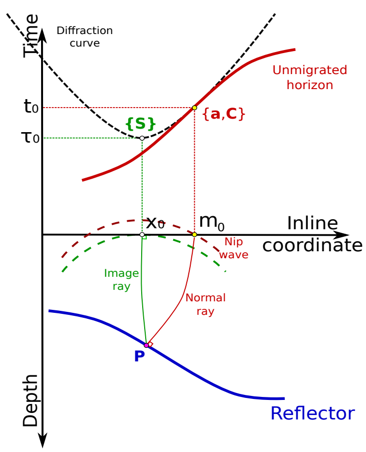

Figure 1: 2D model with a single reflector and its zero-offset (ZO) response in time. Left: Starting at point P on the reflector, the image ray, highlighted in green, and its corresponding normal ray, highlighted in red are shown. The image and normal rays emerge at the measurement surface at $\mathbf{x}_0$ and $\mathbf{m}_0$, respectively. Also shown are the wavefronts of the NIP wave from P as it arrives at $\mathbf{m}_0$ and $\mathbf{x}_0$ in different times. Note that the wavefront is tangent to the measurement surface. In the time domain, the diffraction curve from P is tangent to reflection curve at the ZO trace at $\mathbf{m}_0$. The CRS parameters on that point are $\{\mathbf{a},\mathbf{C}\}$. The same curve has its apex on the ZO trace at $\mathbf{x}_0$. The corresponding parameter at that point is $\mathbf{S}$.

Geometrical interpretation of $t_M(\mathbf{m},\mathbf{h};\mathbf{x}_0,\tau_0)$

The time-migration traveltime of Equations (14)-(16) admit the following appealing interpretation: Consider the isochrone in depth domain specified by the central point $(\mathbf{m}_0, t_0)$. That isochrone is taken only conceptually because we do not have a depth-velocity model. For any point, P, on that isochrone, specified by the lateral coordinate, $\mathbf{x}_0$, and for every fixed half-offset, $\mathbf{h}$, Equation (14) represents the (DSR) traveltime that refers to the point diffractor at P under the common-offset configuration of half-offset, $\mathbf{h}$.

For varying point diffractors along the isochrone, as specified by correspondingly varying coordinate vectors, $\mathbf{x}_0$, an ensemble of diffraction surfaces is obtained. Also under the same common-offset configuration specified by $\mathbf{h}$, such ensemble has, as an envelope, the reflection response of the isochrone, taken as a reflector. In order to determine the envelope of the ensemble of diffraction surfaces parameterized by $\mathbf{x}_0$, we apply the *envelope condition*

$$\frac{\partial t_M}{\partial \mathbf{x}_0}(\mathbf{m},\mathbf{h};\mathbf{x}_0,\tau_0) = \mathbf{0}\,. \qquad (17)$$

Using Equation (12) to replace τ_0^2 and isolating $\mathbf{x}_0$ in the Equation (17), we obtain

$$\mathbf{x}_0 = \mathbf{m}_0 + \frac{4t_0^2\mathbf{S}^{-1}\Delta\mathbf{m}}{\mathbf{h}^T\mathbf{h} - \Delta\mathbf{m}^T\Delta\mathbf{m}}\,. \qquad (18)$$

Substitution of Equations (12) and (18) into Equations (15) and (16), we find the expression

$$[t_R(\mathbf{m},\mathbf{h};\mathbf{m}_0,t_0)]^2 = \mathbf{h}^T\mathbf{S}\mathbf{h} + \frac{t_0^2\mathbf{h}^T\mathbf{h}}{\mathbf{h}^T\mathbf{h} - \Delta\mathbf{m}^T\Delta\mathbf{m}}\,. \qquad (19)$$

Geometrical interpretation of $t_R(\mathbf{m},\mathbf{h};\mathbf{m}_0,t_0)$:

Consider a fixed half-offset, $\mathbf{h}$. Equation (19) represents the reflection traveltime, under the common-offset configuration of half-offset, $\mathbf{h}$, of the ZO isochrone that refers to the central point, $(\mathbf{m}_0,t_0)$, that isochrone taken as a depth reflector. Suppose now that the ZO reflection traveltimes, of the target reflector, as a function of midpoint, $\mathbf{m}_0$, is given by the expression $t_0 = t_0(\mathbf{m}_0)$. For varying points $(\mathbf{m}_0,t_0(\mathbf{m}_0))$ on that reflection curve, the traveltime functions of Equation (19) constitute an ensemble of reflection traveltimes of isochrones, parameterized by the midpoints, $\mathbf{m}_0$. The envelope of that ensemble is obtained by the envelope condition

$$\frac{\partial t_R}{\partial \mathbf{m}_0}(\mathbf{m},\mathbf{h};\mathbf{m}_0,t_0) = 0\,. \qquad (20)$$

Under the consideration that

$$\frac{\partial t_R}{\partial \mathbf{m}_0} = \frac{1}{2t_R}\frac{\partial t_R^2}{\partial \mathbf{m}_0}\,, \qquad (21)$$

we find

$$2\mathbf{a}(\mathbf{h}^T\mathbf{h} - \Delta\mathbf{m}^T\Delta\mathbf{m}) + t_0\Delta\mathbf{m} = \mathbf{0}. \qquad (22)$$

The above quadratic equation in $\Delta\mathbf{m}$ has the solution, $\Delta\mathbf{m} = \Delta\mathbf{m}_{CRP} = \mathbf{m}_{CRP} - \mathbf{m}_0$, where

$$\mathbf{m}_{CRP} = \mathbf{m}_{CRP}(\mathbf{h}) = \mathbf{m}_0 + \frac{2(\mathbf{h}^T\mathbf{a})\mathbf{h}}{t_0 + \sqrt{t_0^2 + 4(\mathbf{h}^T\mathbf{a})^2}}\,. \qquad (23)$$

CRP curve and CRP surface:

In what follows, we assume that the quantities $\{\mathbf{m}_0, t_0, \mathbf{a}, \mathbf{C}\}$ are given. That differs from the usual practice with the CRS method, in which the central point, $(\mathbf{m}_0, t_0)$ is given and the CRS parameters $\mathbf{a}$ and $\mathbf{C}$ are estimated from the data and attached to that central point. Here, the four parameters $\{\mathbf{m}_0, t_0, \mathbf{a}, \mathbf{C}\}$ are all freely given. At a later stage, these four parameters will be estimated regarding their relationship to a given central point $(\mathbf{x}_0, \tau_0)$ in the time-migrated domain.

We recall that the CRP gather that pertains to a given central point, $(\mathbf{m}_0, t_0)$, assumed to be a reflection point in the ZO (stacked) volume, consists of the source-receiver pairs, $(S_{CRP}(\mathbf{h}), G_{CRP}(\mathbf{h}))$ which, for varying half-offsets, $\mathbf{h}$, share the same reflection point at the target reflector. That point is the normal-incident-point (NIP) determined by $(\mathbf{m}_0, t_0)$. The quantities $\{\mathbf{m}_0, t_0, \mathbf{a}, \mathbf{C}\}$, determine the source $S_{CRP}(\mathbf{h}) = \mathbf{m}_{CRP}(\mathbf{h}) - \mathbf{h}$ and receiver $G_{CRP}(\mathbf{h}) = \mathbf{m}_{CRP}(\mathbf{h}) + \mathbf{h}$, in which the midpoints $\mathbf{m}_{CRP}(\mathbf{h})$, is given by Equation (23).

The CRP traveltime curve, $t_{CRP}(\mathbf{h})$ (see Figure 2) that refers to the quantities $\{\mathbf{m}_0, t_0, \mathbf{a}, \mathbf{C}\}$ is chosen to be the one that results from the DSR traveltime applied to the CRP gather that corresponds to such quantities. In symbols

$$t_{CRP}(\mathbf{h}) = t_M(\mathbf{m}_{CRP}(\mathbf{h}), \mathbf{h}) \ . \tag{24}$$

For varying $\mathbf{m}$ in the neighborhood of $\mathbf{m}_0$ and small varying $\mathbf{h}$, the CRP stacking surface, $T_{CRP}(\mathbf{m}, \mathbf{h})$ (see Figure 2) that refers to the central point, $(\mathbf{m}_0, t_0)$, in the ZO (stacked) domain is chosen to be,

$$T_{CRP}(\mathbf{m}, \mathbf{h}) = t_{CRP}(\mathbf{h}) + [\mathbf{a}_{CRP}(\mathbf{h})]^T [\mathbf{m} - \mathbf{m}_{CRP}(\mathbf{h})] \ , \tag{25}$$

with

$$\mathbf{a}_{CRP}(\mathbf{h}) = \frac{\partial t_M}{\partial \mathbf{m}}(\mathbf{m}_{CRP}(\mathbf{h}), \mathbf{h}) \ . \tag{26}$$

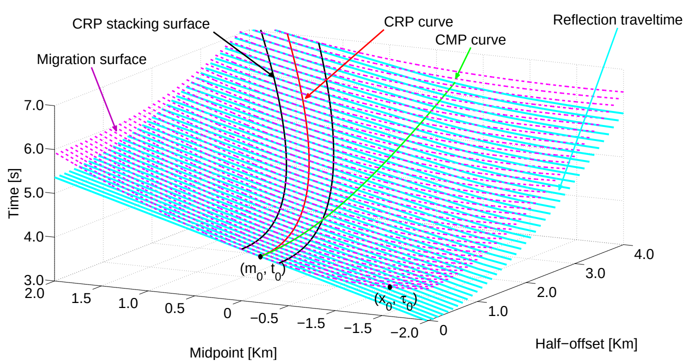

Figure 2: 2D synthetic example of a CRP curve that refers to (m_0, t_0) for a dipping plane reflector. Note that the CRP curve follows the migration surface (starting at (x_0, τ_0)) along the offsets and is also tangent to the reflection traveltime (CRP stacking surface). In contrast, the CMP curve was not able maintain that good fit for increasing offsets.

CRP time migration algorithm

Our aim now is to apply the previous results to construct a CRP time migration traveltime, $t^M_{CRP} = t^M_{CRP}(\mathbf{h})$, and CRP time migration surface, $T^M_{CRS} = T^M_{CRS}(\mathbf{m}, \mathbf{h})$ that refer to a given (central) image point, $(\mathbf{x}_0, \tau_0)$, in the time-migrated domain. For that, we need to estimate the quantities, $\{\mathbf{m}^M_0, t^M_0, \mathbf{a}_M, \mathbf{C}_M\}$, that pertain to the given $(\mathbf{x}_0, \tau_0)$ in the time-migrated domain.

From Equations (8)-(9), we readily see that

$$\begin{aligned} \mathbf{m}^M_0 &= \mathbf{x}_0 + \tau_0 \left[1 - \mathbf{a}^T_M \mathbf{S}^{-1}_M \mathbf{a}_M\right]^{-1/2} (\mathbf{S}^{-1}_M \mathbf{a}_M) \ , \\ t^M_0 &= \tau_0 \left[1 - \mathbf{a}^T_M \mathbf{S}^{-1}_M \mathbf{a}_M\right]^{-1/2} \ , \end{aligned} \tag{27}$$

where we used the notation

$$\mathbf{S}_M = \mathbf{a}_M \, \mathbf{a}^T_M + \mathbf{C}_M \ . \tag{28}$$

From Equations (27), we readily see that our problem reduces to find the parameter pair $(\mathbf{a}_M, \mathbf{C}_M)$. Once these quantities are obtained, the sought-for CRP curve and surface are given by

$$\begin{aligned} t^M_{CRP}(\mathbf{h}) &= t_{DSR}(\mathbf{m}^M_{CRP}(\mathbf{h}), \mathbf{h}) \ , \\ T^M_{CRP}(\mathbf{m}, \mathbf{h}) &= t^M_{CRP}(\mathbf{h}) + [\mathbf{a}^M_{CRP}(\mathbf{h})]^T [\mathbf{m} - \mathbf{m}^M_{CRP}(\mathbf{h})] \ , \end{aligned} \tag{29}$$

where $\mathbf{m}^M_{CRP}$ and $\mathbf{a}^M_{CRP}$ are the same functions as their counterparts $\mathbf{m}_{CRP}$ and $\mathbf{a}_{CRP}$, computed, however, with the quantities $\{\mathbf{m}^M_0, t^M_0, \mathbf{a}_M, \mathbf{C}_M\}$.

Time migration parameter estimation

We are now ready to address the problem of estimating the parameters $\mathbf{a}_M$ and $\mathbf{C}_M$, from which the central point, $(\mathbf{m}^M_0, t^M_0)$, as well as the CRP curve, $t^M_{CRP}(\mathbf{h})$, and CRP surface, $T^M_{CRP}(\mathbf{m}, \mathbf{h})$, are obtained. That is simply done as follows: For a user-selected ensemble of trial parameters $\{\mathbf{a}, \mathbf{C}\}$, construct for each of them the CRP surface, $T_{CRP}(\mathbf{m}, \mathbf{h})$ and compute the stacking energy (semblance) along that surface. The parameter pair for which the maximum energy is attained is the one to be selected.

The estimations indicated above require proper apertures in midpoint and half-offset directions. The aperture in midpoint direction is attached to the estimation of the midpoint inclination, $\mathbf{a}^M_{CRP}$, of the CRP surface for varying offsets. Since $\mathbf{a}$ is the first derivative in midpoint, only a small aperture is needed. In our 2D experiments, we found that aperture sizes of five traces for each offset are enough. Based on these results, in the 3D case, we recommend the same aperture size in inline and crossline directions (i.e., totaling 25 traces in regular grid for each offset). In the half-offset direction, the aperture should be the same as in any prestack time migration. Thus, in the 3D case, the number of traces considered on each estimation of $\mathbf{a}_M$ and $\mathbf{C}_M$ is the number of midpoint traces times the number of offsets.

Computation of CRP time migration

As earlier indicated, we propose a Kirchhoff-type time migration such that, for each output image point, stacks the prestack data along the CRP surface that corresponds to that point. In analogy of the well-established Kirchhoff depth migration (see, e.g., Schleicher et al., 1993), the CRP time migration is computed by an expression of the form

$$D^M_{CRP}(\mathbf{x}_0, \tau_0) = -\frac{1}{2\pi} \int_{\mathscr{A}} W^M_{CRP} \, [\partial_t D]_{t = t^M_{CRP}} \, d\mathbf{m} d\mathbf{h} \ . \tag{30}$$

Here, $D^M_{CRP}(\mathbf{x}_0, \tau_0)$ is the time migration output at the image point, $(\mathbf{x}_0, \tau_0)$, $D = D(\mathbf{m}, \mathbf{h}, t)$ is the prestack data. As well known (see, e.g., Schleicher et al., 1993), the partial derivative of the data, $\partial_t D(\mathbf{m}, \mathbf{h}, t)$ with respect to time is applied to preserve the original time shape of the seismic signal. Moreover, $t^M_{CRP} = t^M_{CRP}(\mathbf{m}, \mathbf{h})$ represents the CRP surface that refers to the (output) image point.

The quantity W^M_{CRP} represents the weight function that aims in the recovering of amplitudes. Based on Zhang et al. (2000), we use the true-amplitude weight for a locally homogeneous medium of matrix migration velocity determined by the matrix $\mathbf{S}$ (see Equation (13)),

$$W^M_{CRP} = \frac{\tau_0\sqrt{|\det\mathbf{S}|}}{4(\delta_h)^2}\left(\frac{1}{t_S}+\frac{1}{t_G}\right)\left(\frac{t_S}{t_G}+\frac{t_G}{t_S}\right), \qquad (31)$$

to measure the amplitudes stacked along of the diffraction manifold in Equation (30). The values t_S and t_G are defined by Equations (15) and (16), respectively.

The migration aperture, denoted $\mathscr{A}$ represents the region over which the migration integral is performed. Based on the concept of Projected Fresnel Zone (PFZ) (Schleicher et al., 1997), the aperture $\mathscr{A}$ is proposed to consist of points $(\mathbf{m},\mathbf{h})$ which simultaneously satisfy the conditions

$$\|\mathbf{m}-\mathbf{m}_{CRP}(\mathbf{h})\| < \delta_m \quad \text{and} \quad \|\mathbf{h}\| < \delta_h\,, \qquad (32)$$

where, δ_m and δ_h are midpoint and half-offset aperture bounds. Here, the aperture bound in half-offset direction, δ_h, is taken as the one used in any prestack time migration. Following the same lines as in Faccipieri et al. (2015), the aperture bound in midpoint direction, δ_m can be given by

$$\delta_m = \alpha\sqrt{\frac{w t_0^M}{\lambda_C}}\,, \qquad (33)$$

where, $|\lambda_C| = \max\{|\lambda_{C1}|,|\lambda_{C2}|\}$, in which λ_{C1} and λ_{C2} are the eigenvalues of the 2×2 symmetric matrix $\mathbf{C}$, w is the length of the seismic pulse. Moreover, t_0^M is the ZO traveltime that is given by Equation (27), in terms of the CRS parameters, $\{\mathbf{a}_M,\mathbf{C}_M\}$, that pertain to the (output) image point $(\mathbf{x}_0,\tau_0)$. Finally, $\alpha > 1$ is a user-selected adjustment parameter.

Examples

The proposed CRP time migration was applied to a 2D real dataset acquired offshore in Brazil at Jequitinhonha basin. The dataset has 4 ms time sampling, 12.5 m between Common Midpoint (CMP) gathers, 25 m between hydrophones with minimum and maximum offsets of 150 m and 3125 m, respectively. For comparison purposes, Figure 3 (top) shows a CRS stacked section obtained with global estimation of parameters with the following apertures: (i) Midpoint: 30 m from zero to 1.3 s, increasing linearly until 150 m at 3.5 s and constant until the maximum time sample. (ii) Offset: 650 m from 0 to 1.3 s, increasing linearly until 1050 m at 3.5 s and constant until the final time, 6.0 s. A conventional post-stack Kirchhoff time-migrated section constructed with that dataset is shown at Figure 3 (bottom). The migration aperture that has been used was ten times greater than the proposed minimum aperture, i.e., $\alpha = 10$ in Equation (33). We observe that, under that conventional procedure, smaller apertures were not able to image some of the dips present in the data. To carry out the CRP time migration, the CRS parameters a and C needed to be estimated using T^M_{CRP} from Equation (29). In the present example, the estimations were performed using constant midpoint and half-offset apertures of 50 m and 1000 m, respectively. Once these parameters were estimated, for each (x_0,τ_0), the dataset was time migrated, considering a 2.5D case formulation. The obtained time-migration section is shown in Figure 4 (top). The migration apertures were calculated using Equation (33) for each (m_0^M,t_0^M) with $\alpha = 1$ and

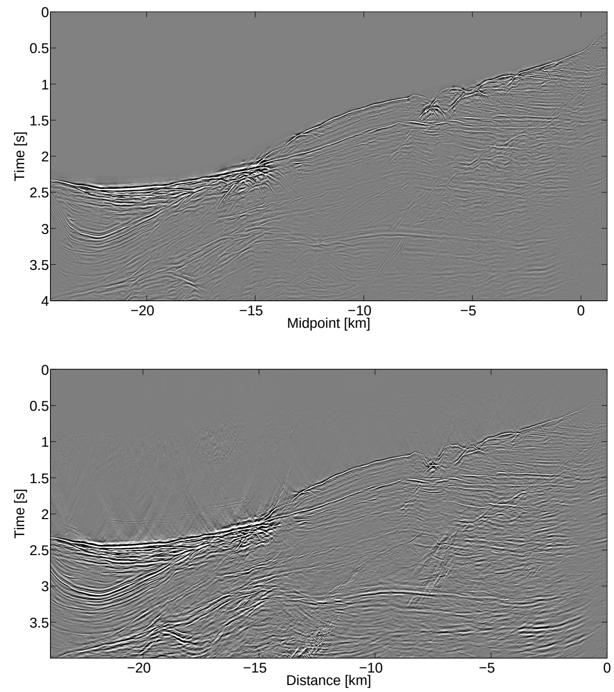

Figure 3: Stacked section obtained with CRS method (top) and its post-stack Kirchhoff migration with aperture ten times ($\alpha = 10$) than the proposed minimum aperture in midpoints (bottom). Remark: the velocity model used to migrate the dataset was obtained by the CRP time migration.

$w = 40$ ms which leads to different values of apertures depending of C_M and t_0^M. Figure 4 (bottom) shows the semblance values for the estimated parameters. It is possible to identify and quantify the regions where the CRP surface adjusted the events properly. The semblance panel can be seen as a valuable tool for the purposes of evaluation and quality control of the CRP time migration. Figure (5) shows the estimated parameter a and S, converted on angles and velocities for illustrative purposes, for each (x_0,τ_0)

Conclusions

A Kirchhoff-type, time migration algorithm is proposed that is optimal in two respects. First, the summation is performed along the common-reflection-point (CRP) curve (as opposed to the conventional diffraction-time hyperbola). Second, a small aperture, associated to the projected Fresnel zone (PFZ), is employed that is able to restrict the summation to that part of the CRP curve where constructive interference occurs. A key feature of the algorithm is a transformation function that maps each given image point into a corresponding point in the zero-offset (ZO) (stacked) volume and also computes the ZO common-reflection-surface (CRS) parameters there. Such quantities are used to construct the CRP curve and the summation aperture at each image point. First field-data examples confirm the good potential of the new technique for high-quality, time migration results.

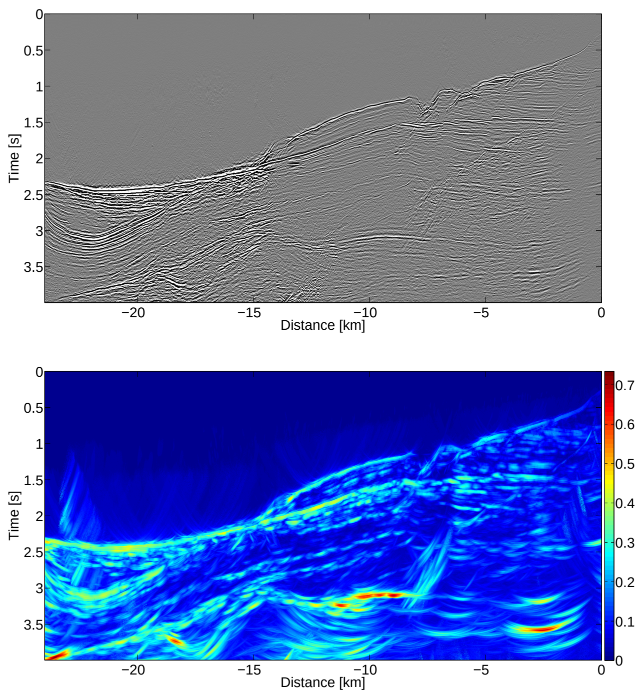

Figure 4: Top: Prestack time-migrated obtained with the proposed CRP algorithm using the minimum apertures in midpoints. Bottom: Semblance values obtained on the estimation of parameters for each (x_0, τ_0).

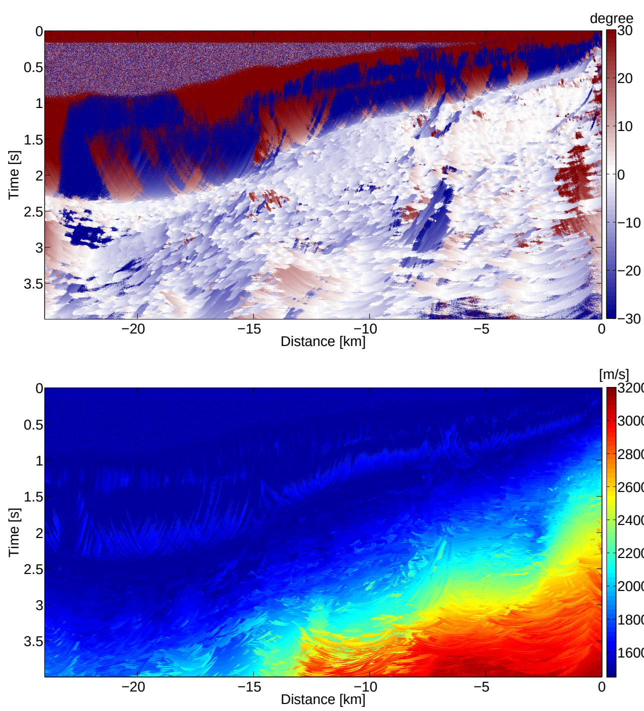

Figure 5: Parameter a converted in degrees (top) and parameter S converted in velocities (bottom) obtained for each (x_0, τ_0).

Acknowledgments

We acknowledge support from the National Council for Scientific and Technological Development (CNPq-Brazil), the National Institute of Science and Technology of Petroleum Geophysics (ICTP-GP-Brazil) and the Center for Computational Engineering and Sciences (Fapesp/Cepid # 2013/08293-7-Brazil). We also acknowledge support of the sponsors of the Wave Inversion Technology (WIT) Consortium.

References

Cameron, M. K., S. B. Fomel, and J. A. Sethian, 2007, Seismic velocity estimation from time migration: Inverse Problems, **23**, 1329–1369.

Coimbra, T. A., A. Novais, and J. Schleicher, 2011, Offset continuation (OCO) ray tracing using OCO trajectories: Stud Geophys Geod, **56**, 65–82.

——–, 2013, Theory of offset-continuation trajectory stack: Presented at the 13th International Congress of the Brazilian Geophysical Society & EXPOGEF, Rio de Janeiro, Brazil, 26–29 August 2013, Society of Exploration Geophysicists and Brazilian Geophysical Society.

Dell, S., D. Gajewski, and M. Tygel, 2014, Image ray tomography: Geophysical Prospecting, **62**, 413–426.

Faccipieri, J. H., T. A. Coimbra, L. J. Gelius, and M. Tygel, 2015, Bi-parametric traveltimes and stacking apertures for reflection and diffrection enhancement: Submitted: 14th International Congress of the Brazilian Geophysical Society (SBGf) , Rio de Janeiro.

Gelius, L.-J., and M. Tygel, 2015, Migration-velocity building in time and depth from 3D (2D) common-reflection-surface (CRS) stacking - theoretical framework: Stud Geophys Geod.

Hubral, P., and T. Krey, 1980, Interval velocities from seismic reflection time measurements: SEG.

Iversen, E., and M. Tygel, 2008, Image-ray tracing for joint 3D seismic velocity estimation and time-to-depth conversion: Geophysics, **73**, S99–S114.

Mann, J., P. Hubral, B. Traub, A. Gerst, and H. Meyer, 2000, *in* Macro-model independent approximative prestack time migration: EAGE, Expanded Abstracts, 62nd Mtg. Eur. Assn. Geosci. Eng.

Perroud, M., P. Hubral, and G. Höcht, 1999, Common-reflection-point stacking in laterally inhomogeneous media: Geophysical Prospecting, **47**, 1–24.

Schleicher, J., P. Hubral, M. Tygel, and M. S. Jaya, 1997, Minimum apertures and Fresnel zones in migration and demigration: Geophysics, **62**, 183–194.

Schleicher, J., M. Tygel, and P. Hubral, 1993, 3-D true-amplitude finite-offset migration: Geophysics, **58**, 1112–1126.

Spinner, M., and J. Mann, 2006, True-amplitude based Kirchhoff time migration for AVO/AVA analysis: J. Seis. Expl., **15**, 133–152.

Yilmaz, O., 2001, Seismic data analysis: Processing, inversion and interpretation of seismic data (2nd edition): Society of Exploration Geophysicists (SEG), Oklahoma, Tulsa, USA.

Zhang, Y., S. Gray, and J. Young, 2000, Exact and approximate weights for Kirchhoff migration: Presented at the SEG Technical Program Expanded Abstracts 2000, Society of Exploration Geophysicists.